Fingerprints of a position-dependent Fermi velocity on scanning tunnelling spectra of strained graphene

IOP Publishing Journal of Physics: Condensed Matter
J. Phys.: Condens. Matter **30** (2018) 085702 (6pp) https://doi.org/10.1088/1361-648X/aaa7b3

Fingerprints of a position-dependent Fermi velocity on scanning tunnelling spectra of strained graphene

M Oliva-Leyva[1], J E Barrios-Vargas[2] and Chumin Wang[1]

[1] Instituto de Investigaciones en Materiales, Universidad Nacional Autónoma de México, Apartado Postal 70-360, 04510 Mexico City, Mexico
[2] Departamento de Física, Facultad de Ciencias Físicas y Matemáticas, Universidad de Chile, Santiago, Chile

E-mail: mauriceoliva.cu@gmail.com, j.e.barrios@gmail.com and chumin@unam.mx

Received 19 October 2017, revised 27 December 2017
Accepted for publication 15 January 2018
Published 1 February 2018

Abstract

Nonuniform strain in graphene induces a position dependence of the Fermi velocity, as recently demonstrated by scanning tunnelling spectroscopy experiments. In this work, we study the effects of a position-dependent Fermi velocity on the local density of states (LDOS) of strained graphene, with and without the presence of a uniform magnetic field. The variation of LDOS obtained from tight-binding calculations is successfully explained by analytical expressions derived within the Dirac approach. These expressions also rectify a rough Fermi velocity substitution used in the literature that neglects the strain-induced anisotropy. The reported analytical results could be useful for understanding the nonuniform strain effects on scanning tunnelling spectra of graphene, as well as when it is exposed to an external magnetic field.

Keywords: graphene, strain, scanning tunnelling spectroscopy, position-dependent Fermi velocity, magnetic field

(Some figures may appear in colour only in the online journal)

Unlike most of the crystals, graphene can be reversibly stretched beyond 10%. This unusual elastic response has made it suitable to modify its electronic and optical properties via strains, idea known as strain engineering [1, 2]. For instance, when graphene is uniformly deformed, its low-energy electronic band structure around the Dirac points becomes elliptical cones. This fact can be visualized as an anisotropy of the Fermi velocity [3]. As a consequence, the optical conductivity of graphene under uniform strain results anisotropic [4, 5], which produces a modulation of the optical transmittance as a function of the incident light polarization [6, 7]. This strain sensitivity of the optical response of graphene has been experimentally observed [8] and, as proposed, it could be utilized towards the design of novel ultra-thin optical devices and strain sensors [9]. Furthermore, it has been recently shown that the Faraday (Kerr) effect in graphene can be modified by means of deformations [10].

Nonuniform strains constitute even more useful tools to archive new behaviors of graphene. For example, the emergence of a pseudomagnetic field caused by a nonuniform strain can produce a pseudoquantum Hall effect in absence of external magnetic field [11, 12]. Nowadays, signatures of such gauge field in the electronic transport properties of graphene are actively investigated [13–18]. Moreover, nonuniform strains graphene opens new opportunities to investigate others striking behaviors such as fractal spectrum [19], metal-insulator transition [20], superconducting states [21] and magnetic phase transitions [22]. Within the Dirac approximation, in addition to the mentioned pseudomagnetic field, nonuniform strains give rise another recognized effect: a position-dependent Fermi velocity (PDFV) [23]. However, signatures of PDFV in the graphene physics have been less addressed, even though they are always present for any nonuniform strain.

Given that scanning tunnelling spectroscopy (STS) spectra provide the local density of states (LDOS), which depends on the Fermi velocity v_0 as $\rho_0(E) \sim |E|/v_0^2$ for pristine graphene, the slopes of V-shaped STS spectra present variations at different positions of the sample if the Fermi velocity is spatially varying. Based on this idea, evidence of the PDFV effect in strained graphene has been provided in a few experiments through STS [24, 25]. However, to obtain a local measurement of the Fermi velocity, typically v_0 is replaced by $v(x)$ in $\rho_0(E)$ leading to $\rho(E,x) \sim |E|/v^2(x)$, where x is the measured position across the strain direction. According to this substitution, Fermi velocities at two different positions, $v(x_1)$ and $v(x_2)$, are related by the expression, $v(x_1)/v(x_2) = [\mathcal{S}(x_2)/\mathcal{S}(x_1)]^{1/2}$, where $\mathcal{S}(x)$ is the STS spectrum slope at the position x [25]. A purpose of this work is to clarify that the appropriate expression is given by $v(x_1)/v(x_2) = \mathcal{S}(x_2)/\mathcal{S}(x_1)$, at least when a space dependent Fermi velocity is due to a nonuniform uniaxial strain.

From the quantum field theory it has been pointed out that a PDFV (in curved graphene) becomes spatial modulations of LDOS [26]; nevertheless, a better description of strain-induced PDFV has been arrived at from low-energy expansions of the standard tight-binding model [23, 27–29]. The achievement of these last studies consists of determining the Fermi velocity tensor as a function of the position-dependent strain tensor. This fact has allowed to approximately calculate within the Dirac model the PDFV effect on the LDOS and, therefore, on STS measurements. However, the analytical expressions for the LDOS of strained graphene, reported in [27], have not been compared with results obtained from tight-binding calculations. Such a comparison will be presented in this article.

Moreover, STS experiments in the presence of a magnetic field can also be used to reveal local variations of the Fermi velocity, as performed in randomly strained graphene [30] as well as on the surface of a complex topological insulator [31]. Here, we report the first detailed study, to our best knowledge, of the PDFV effect on Landau-level spectroscopy using both approaches, tight-binding model and Dirac approximation, in order to provide a better understanding and a more complete theoretical framework for these types of experiments carried out in strained graphene under an external magnetic field.

1. PDFV effect on LDOS

For graphene, the electronic implications of strain can be investigated by means of the nearest-neighbor tight-binding Hamiltonian

$$\mathcal{H} = -\sum_{\langle i,j\rangle} t_{ij} c_i^\dagger c_j, \tag{1}$$

where the sum $\langle i,j\rangle$ runs over nearest neighbors and $c_i^\dagger$ (c_i) is the creation (annihilation) field operator at the ith site. The strain-induced modification of the nearest-neighbor hopping parameter t_{ij} is captured by [32]

$$t_{ij} = t_0 \exp[-\beta(d_{ij}/a_0 - 1)], \tag{2}$$

where $t_0 = 2.7$ eV, $\beta = 3.37$, $a_0 = 0.142$ nm is the interatomic distance for unstrained graphene, and d_{ij} is the modified distance between atomic sites i and j. It is relevant for the present discussion to note that the Hamiltonian (1) with constant t_{ij} is not capable to describe purely geometric effects on LDOS induced by nonuniform strain [23]. For example, if one assumes $\beta = 0$, equation (1) becomes $\mathcal{H} = -t_0 \sum_{\langle i,j\rangle} c_i^\dagger c_j$ which has the same eigenenergies and eigenfunctions of pristine graphene even when the atoms move from their equilibrium positions.

In order to isolate PDFV effects, we consider a nonuniform uniaxial strain along the zigzag crystalline orientation, as shown in figure 1(a), which is generated by a displacement field of the form $\boldsymbol{u}(x,y) = u_0 \sin(2\pi x/\lambda)\boldsymbol{e}_x$, with $\boldsymbol{e}_x$ being the unit vector in the x-direction. The parameters λ and u_0 fulfill conditions $a_0/\lambda \ll 1$ and $2\pi u_0/\lambda \ll 1$, allowing the comparison between discrete and continuous models. In fact, this particular nonuniform strain does not produce pseudomagnetic field B_s. Because according to the considered displacement field $\boldsymbol{u}$, the components of the strain tensor defined by $\epsilon_{ij} = (\partial_i u_j + \partial_j u_i)/2$ result $\epsilon_{xx}(x) = (2\pi u_0/\lambda)\cos(2\pi x/\lambda)$ and $\epsilon_{yy} = \epsilon_{xy} = 0$; at the same time B_s is related to the strain tensor through $B_s \sim (\partial_y \epsilon_{xx} - \partial_y \epsilon_{yy} + 2\partial_x \epsilon_{xy})$ [11], therefore $B_s = 0$. It is worth noting that for an out-of-plane displacement field $h(x)$, e.g. a ripple along the zigzag direction, the physical situation is essentially the same as that studied here, since one has only PDFV effects within the linear approximation [29].

Within the tight-binding model, we calculate the LDOS at the atomic site n through $\rho(E,n) = (-1/\pi)\mathrm{Im}[G^+(n,n;E)]$, where $G^+(n,m;E)$ is the retarded Green's function evaluated using a uniform Monkhorst-Pack grid[3]. Given the considered displacement field, the LDOS depends only the x-coordinate and, besides, it results λ-periodic if λ is a multiple of $\sqrt{3}a_0$.

Figure 1(b) shows the LDOS at low energies, for $\lambda = 660\sqrt{3}a_0$ and $2\pi u_0 = 0.1\lambda$, at three distinct sites of the strained graphene sample which are labelled as x_1, x_2 and x_3, respectively. At x_1 the sample has a maximum local stretching along the zigzag direction of 10% ($\epsilon_{xx} = 0.1$), whereas that at x_3 it has a maximum local shrinking of 10% ($\epsilon_{xx} = -0.1$). In contrast, at x_2 the local strain is close to zero ($\epsilon_{xx} \approx 0$). This change of strain along of the zigzag direction induces a variation of the LDOS observed in figure 1(b). In brief, the V-shape of LDOS at low energies is more widely-opened in the shrinked region than in the stretched one.

This behavior is quantitatively registered by figure 1(c), where we present the positive slope of the V-shaped LDOS $\mathcal{S}(x)$, in units of the slope $\mathcal{S}_0$ for unstrained graphene, as a function of the position x from three different approaches. The open circles correspond to our tight-binding calculations of $\mathcal{S}(x)$, whereas the solid circles are given by $\mathcal{S}(x) = \mathcal{S}_0/[1 - \beta\epsilon_{xx}(x)]$, according to the Dirac approach [27]. Good agreement is observed for these two approaches, confirming that the LDOS variation is indeed induced by PDFV.

[3] We set the Monkhorst-Pack grid-spacing equal to 0.0013 Å^{-1}.

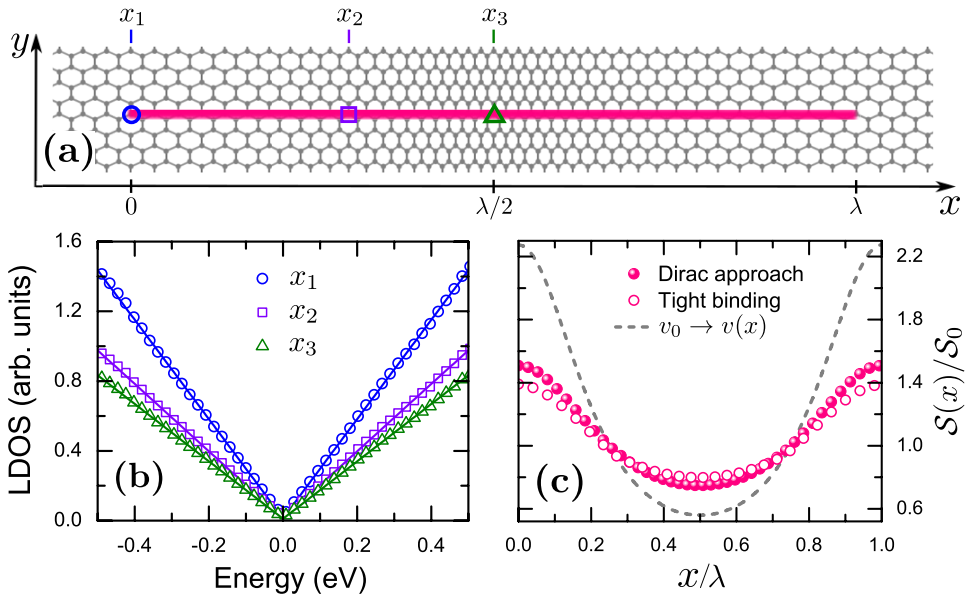

Figure 1. (a) Schematic representation of an oscillating displacement field with wavelength λ along the zigzag direction of graphene. (b) Tight-binding results of the LDOS at three positions illustrated in panel (a). Solid lines obtained from fitting indicate the LDOS slope, $\mathcal{S}(x)$, at distinct sites. (c) Strain-induced variation of positive $\mathcal{S}(x)$ along the pink path in panel (a), according to three different approaches denoted in the figure. Results of panels (b) and (c) are obtained for $\lambda = 660\sqrt{3}a_0$ and $2\pi u_0 = 0.1\lambda$.

Let us explain the essence of the analytical expression derived within the Dirac approximation. For graphene under uniform strain, i.e. non-position dependent strain, the LDOS results $\rho(E) = \rho_0(E)/\det(v_{ij}/v_0)$, where $v_{ij} = v_0(1 - \beta\epsilon_{ij} + \epsilon_{ij})$ is the strain-induced Fermi velocity tensor [5] whose β-independent term $v_0\epsilon_{ij}$ is purely a geometric consequence due to the lattice deformation [29]. Then for a sufficiently smooth spatially-varying strain, the LDOS can be approximately calculated by making the substitution $\epsilon_{ij} \rightarrow \epsilon_{ij}(x, y)$. In consequence, for our problem $\rho(E, x) = \rho_0(E)/[1 - \beta\epsilon_{xx}(x) + \epsilon_{xx}(x)]$, but disregarding geometric effects (given by the β-independent term) in order to compare with the tight-binding results, one finally get $\mathcal{S}(x) = \mathcal{S}_0/[1 - \beta\epsilon_{xx}(x)]$.

In other words, the considered strain only modifies the Fermi velocity in the x-direction, whereas the Fermi velocity in the y-direction remains equal to v_0. Hence, the substitution $v_0 \rightarrow v(x)$ in $\rho_0(E) = 2|E|/(\pi\hbar^2 v_0^2)$ is not appropriate to obtain $\rho_0(E, x)$ because when making such an substitution, one would be wrongly assuming that both components of the velocity are equally modified by strain. To visualize this fact, in figure 1(c) we illustrate with a dashed line the variation of the slope derived by replacing v_0 in $\rho_0(E)$ by $v_0[1 - \beta\epsilon_{xx}(x)]$, which remarkably differs from the ones obtained from the tight-binding and Dirac approaches. Therefore, to obtain a more accurate LDOS of graphene under a nonuniform uniaxial strain (e.g. a ripple as considered in [25]) the appropriate replacement should be $v_0^2 \rightarrow v_0 v(x)$ in $\rho_0(E)$, where $v(x)$ is the Fermi velocity along the strain direction. In consequence, one gets $\rho(E, x) = \rho_0(E)v_0/v(x)$, whence the LDOS slopes at two different positions, $\mathcal{S}(x_1)$ and $\mathcal{S}(x_2)$, are related by the expression

$$\mathcal{S}(x_1)/\mathcal{S}(x_2) = v(x_2)/v(x_1). \tag{3}$$

2. PDFV effect on LDOS in the presence of magnetic field

We now add a uniform magnetic field $\boldsymbol{B}e_z$ to our previously discussed problem of strained graphene.

Within the tight-binding model, the Hamiltonian has the form (1), but now the hopping parameter t_{ij} is evaluated by a generalized expression of equation (2) as

$$t_{ij} = t_0 \exp[-\beta(d_{ij}/a_0 - 1)] \exp[\mathrm{i}\phi_{ij}], \tag{4}$$

in which the magnetic field effect is introduced by the Peierls phase ϕ_{ij}, according to [33, 34]

$$\phi_{ij} = \frac{2\pi}{\phi_0} \int_{\boldsymbol{r}_i}^{\boldsymbol{r}_j} \boldsymbol{A}(\boldsymbol{r}) \cdot \mathrm{d}\boldsymbol{r}, \tag{5}$$

where ϕ_0 is the magnetic flux quantum, $\boldsymbol{A}(\boldsymbol{r})$ is the vector potential and $\boldsymbol{r}_i$ ($\boldsymbol{r}_j$) denotes the modified position of site i (j). Unlike the case without magnetic field, the tight-binding Hamiltonian in the presence of magnetic field captures purely geometric effects due to strain. Even for $\beta = 0$, the resulting hopping parameter $t_{ij} = t_0 \exp[\mathrm{i}\phi_{ij}]$ depends on the position through the Peierls phase, leading to a spatial modulation of the LDOS.

Figure 2(a) is analogous to figure 1(b), but the shown LDOS were calculated by assuming a magnetic field of magnitude $B = 10\,\mathrm{T}$. The most remarkable feature of figure 2(a) is the presence of a series of well defined peaks. For pristine graphene, the LDOS presents such peaks at the Landau level energies, given by $E_n^{(0)} = \pm\sqrt{2e\hbar v_0^2 Bn}$ [35]. For example, the first (positive) peak is at $E_1^{(0)} \approx 0.1\,\mathrm{eV}$ for $B = 10\,\mathrm{T}$. In figure 2(a) for nonuniformly strained graphene, the first peak of the LDOS, located at energy $\mathcal{E}_1(x)$, is around 0.1 eV but it depends on the position x. For instance, $\mathcal{E}_1(x_1) < 0.1$ eV in

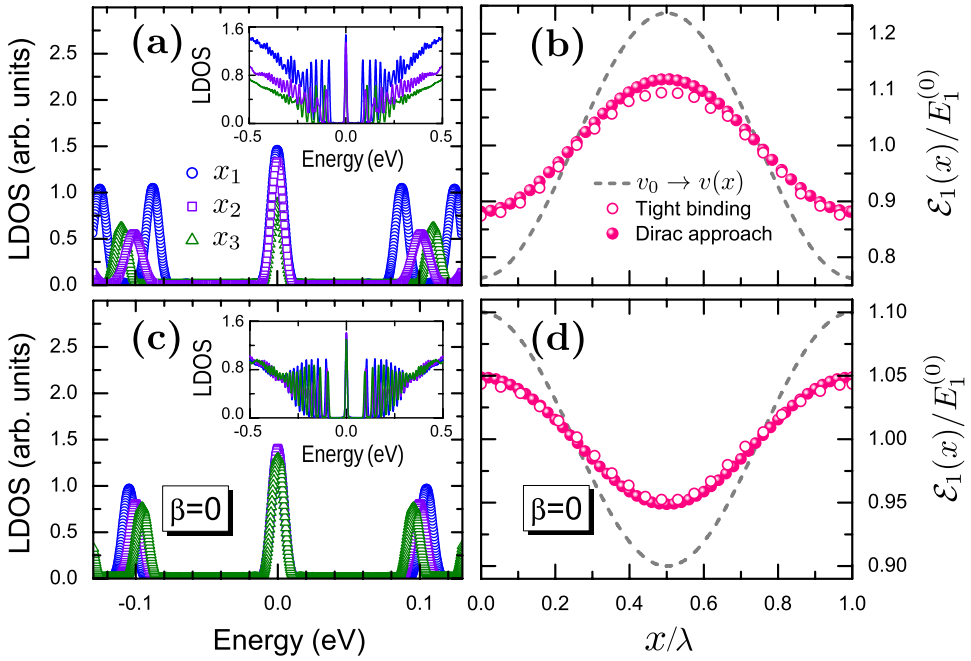

Figure 2. Tight-binding calculations of the LDOS for graphene under a nonuniform uniaxial strain, as illustrated in figure 1(a), and in the presence of a magnetic field B. (a) LDOS at three positions as indicated in figure 1(a) with the corresponding colors. (b) First peak of the LDOS, $\mathcal{E}_1(x)$, as function of the position x along the strain direction, according to three different approaches. Panels (c) and (d) are analogous to panels (a) and (b), respectively, but assuming $\beta = 0$. Insets: LDOS over an extended energy range. Parameters: $\lambda = 660\sqrt{3}a_0$, $2\pi u_0 = 0.1\lambda$ and $B = 10\,\mathrm{T}$.

the stretched region, $\mathcal{E}_1(x_3) > 0.1\,\mathrm{eV}$ in the shrinked region, and $\mathcal{E}_1(x_2) \approx 0.1\,\mathrm{eV}$, where local strain is approximately zero. This variation of $\mathcal{E}_1(x)$ with the position x is quantitatively displayed by open pink circles in figure 2(b), according to our tight-binding calculations. Moreover, to visualize the purely geometric effects due to strain, in figure 2(c) we show the LDOS, as analogously made in figure 2(a), but obtained by assuming $\beta = 0$ in equation (4). For this hypothetical case, the dependence of $\mathcal{E}_1(x)$ as function of x is opposite to that of the realistic case with $\beta = 3.37$, which can be clearly noted by comparing figures 2(b) and (d).

Let us provide an explanation to the tight-binding results of $\mathcal{E}_1(x)$ from the Dirac approximation in terms of PDFV effects on the LDOS. For graphene under uniform strain, the Landau level energies are given by $E_n = E_n^{(0)}\sqrt{\det(v_{ij}/v_0)}$, with $v_{ij} = v_0(1 - \beta\epsilon_{ij} + \epsilon_{ij})$ [10]. Hence, the first peak of the LDOS for uniformly strained graphene should be at $E_1 = E_1^{(0)}[1 - (\beta - 1)\mathrm{tr}(\epsilon_{ij})/2]$, up to first-order in the strain tensor. Then, for a sufficiently smooth spatially-varying strain, $\mathcal{E}_1(x, y)$ can be approximately estimated by making the substitution $\epsilon_{ij} \to \epsilon_{ij}(x, y)$ in E_1, which leads to

$$\mathcal{E}_1(x, y) = E_1^{(0)}\left\{1 - \frac{\beta - 1}{2}\mathrm{tr}[\epsilon_{ij}(x, y)]\right\}. \qquad (6)$$

Thus, at a locally dilated region ($\mathrm{tr}[\epsilon_{ij}(x, y)] > 0$) the first positive peak of the LDOS is shifted to the left of $|E_1^{(0)}|$, whereas at a locally compressed region ($\mathrm{tr}[\epsilon_{ij}(x, y)] < 0$) the first positive peak of the LDOS is shifted to the right.

From equation (6), for a nonuniform strain as illustrated in figure 1(a), it follows that $\mathcal{E}_1(x) = E_1^{(0)}[1 - (\beta - 1)\epsilon_{xx}(x)/2]$. In figure 2(b) with $\beta = 3.37$ and figure 2(d) with $\beta = 0$, it can be observed a good agreement between the results predicted by the last analytical expression, according to the Dirac approach, and those obtained from the tight-binding model. This fact confirms the concept of a PDFV for the understanding and description of LDOS variations induced by a nonuniform uniaxial strain. Moreover, in figures 2(b) and (d) we illustrate by the dashed lines the consequence of substitution $v_0 \to v(x)$ in $E_1^{(0)}$, which leads to results notably different from those obtained by the tight-binding and Dirac approaches. In short, to evaluate approximately $\mathcal{E}_1(x)$ for graphene under a nonuniform uniaxial strain (e.g. a ripple) and in the presence of a uniform magnetic field, the appropriate replacement should be $v_0^2 \to v_0 v(x)$ in $E_1^{(0)}$, hence one gets $\mathcal{E}_1(x) = E_1^{(0)}\sqrt{v(x)/v_0}$, keeping in mind that $v(x)$ is the Fermi velocity along the strain direction. Therefore, using Landau-level spectroscopy measurements, Fermi velocities at two different positions, $v(x_1)$ and $v(x_2)$, are related by

$$v(x_1)/v(x_2) = [\mathcal{E}_1(x_1)/\mathcal{E}_1(x_2)]^2. \qquad (7)$$

Equation (7) is certainly limited to a nonuniform uniaxial strain along the zigzag direction. For a situation beyond uniaxial strain, the PDFV effect on the LDOS peaks can be quantified by a more general expression as equation (6), which is valid whenever the strain-induced pseudomagnetic field $B_s(x, y)$ fulfills the condition $B_s(x, y)/B \ll \mathrm{tr}[\epsilon_{ij}(x, y)]$.

On the other hand, as illustrated in the inset of figure 2(a), the LDOS presents an inclination (slope) over an extended energy range. Furthermore, this inclination depends on the position in the same manner as occurred in figure 1(b), which

can be explained as a PDFV effect. For the case $\beta = 0$, see inset of figure 2(c), the mentioned position dependence of the LDOS inclination is less remarked because the PDFV effect is only introduced through the Peierls phase.

3. Conclusions

In closing, we have presented a numerical and analytical study of the LDOS of graphene under nonuniform uniaxial strain, either in absence or in presence of a uniform magnetic field. Our tight-binding results of the LDOS have been successfully explained by analytical expressions derived from the Dirac approximation in term of a PDFV. Moreover, we have clarified that the replacement $v_0 \to v(x)$ in expressions of pristine graphene (e.g. $\rho_0(E) \sim |E|/v_0^2$) could be inappropriate to evaluate PDFV effects on LDOS since such rough approach disregards the strain-induced anisotropy of the Fermi velocity. In consequence, the analytical expressions (3) and (7) for the LDOS can be useful to appropriately describe effects of nonuniform uniaxial strains (e.g. ripples along the zigzag direction) on STS experiments of graphene, without and with the presence of a uniform magnetic field. It is important to mention that the analytical results reported in this article are valid for $\lambda \gg \ell_B \gg a_0$, where $\ell_B = \sqrt{\hbar/(eB)}$ is the magnetic length. In addition to the contribution of this work for understanding PDFV effects on Landau-level spectroscopy measurements of strained graphene, our results also suggest that PDFV effects should be considered in a complete description of transport signatures of strain-induced pseudomagnetic fields.

Acknowledgments

This work has been partially supported by CONACYT of Mexico through Project 252943, and by PAPIIT of Universidad Nacional Autónoma de México (UNAM) through Project IN106317. Computations were performed at Miztli of UNAM. MOL acknowledges the postdoctoral fellowship from DGAPA-UNAM. JEBV acknowledges support from FondeCyT-Postdoctoral 3170126.

ORCID iDs

M Oliva-Leyva https://orcid.org/0000-0002-4631-772X
Chumin Wang https://orcid.org/0000-0002-2737-9722

References

[1] Amorim B *et al* 2016 Novel effects of strains in graphene and other two dimensional materials *Phys. Rep.* **617** 1–54
[2] Naumis G G, Barraza-Lopez S, Oliva-Leyva M and Terrones H 2017 Electronic and optical properties of strained graphene and other strained 2D materials: a review *Rep. Prog. Phys.* **80** 096501
[3] Oliva-Leyva M and Wang C 2017 Low-energy theory for strained graphene: an approach up to second-order in the strain tensor *J. Phys.: Condens. Matter.* **29** 165301
[4] Pellegrino F M D, Angilella G G N and Pucci R 2010 Strain effect on the optical conductivity of graphene *Phys. Rev.* B **81** 035411
[5] Oliva-Leyva M and Naumis G G 2014 Anisotropic AC conductivity of strained graphene *J. Phys.: Condens. Matter* **26** 125302
[6] Pereira V M, Ribeiro R M, Peres N M R and Neto A H C 2010 Optical properties of strained graphene *Europhys. Lett.* **92** 67001
[7] Oliva-Leyva M and Naumis G G 2015 Tunable dichroism and optical absorption of graphene by strain engineering *2D Mater.* **2** 025001
[8] Ni G-X, Yang H-Z, Ji W, Baeck S-J, Toh C-T, Ahn J-H, Pereira V M and Özyilmaz B 2014 Tuning optical conductivity of large-scale CVD graphene by strain engineering *Adv. Mater.* **26** 1081–6
[9] Bae S-H, Lee Y, Sharma B K, Lee H-J, Kim J-H and Ahn J-H 2013 Graphene-based transparent strain sensor *Carbon* **51** 236–42
[10] Oliva-Leyva M and Wang C 2017 Magneto-optical conductivity of anisotropic two-dimensional Dirac–Weyl materials *Ann. Phys.* **384** 61–70
[11] Guinea F, Katsnelson M I and Geim A K 2010 Energy gaps and a zero-field quantum Hall effect in graphene by strain engineering *Nat. Phys.* **6** 30–3
[12] Guinea F, Geim A K, Katsnelson M I and Novoselov K S 2010 Generating quantizing pseudomagnetic fields by bending graphene ribbons *Phys. Rev.* B **81** 035408
[13] Stegmann T and Szpak N 2016 Current flow paths in deformed graphene: from quantum transport to classical trajectories in curved space *New J. Phys.* **18** 053016
[14] Settnes M, Leconte N, Barrios-Vargas J E, Jauho A-P and Roche S 2016 Quantum transport in graphene in presence of strain-induced pseudo-Landau levels *2D Mater.* **3** 034005
[15] Carrillo-Bastos R, León C, Faria D, Latgé A, Andrei E Y and Sandler N 2016 Strained fold-assisted transport in graphene systems *Phys. Rev.* B **94** 125422
[16] Georgi A *et al* 2017 Tuning the pseudospin polarization of graphene by a pseudomagnetic field *Nano Lett.* **17** 2240–5
[17] Jones G W, Bahamon D A, Castro Neto A H and Pereira V M 2017 Quantized transport, strain-induced perfectly conducting modes, and valley filtering on shape-optimized graphene Corbino devices *Nano Lett.* **17** 5304–13
[18] Settnes M, Garcia J H and Roche S 2017 Valley-polarized quantum transport generated by gauge fields in graphene *2D Mater.* **4** 031006
[19] Naumis G G and Roman-Taboada P 2014 Mapping of strained graphene into one-dimensional Hamiltonians: quasicrystals and modulated crystals *Phys. Rev.* B **89** 241404
[20] Tang H-K, Laksono E, Rodrigues J N B, Sengupta P, Assaad F F and Adam S 2015 Interaction-driven metal-insulator transition in strained graphene *Phys. Rev. Lett.* **115** 186602
[21] Kauppila V J, Aikebaier F and Heikkilä T T 2016 Flat-band superconductivity in strained Dirac materials *Phys. Rev.* B **93** 214505
[22] López-Sancho M P and Brey L 2016 Magnetic phases in periodically rippled graphene *Phys. Rev.* B **94** 165430
[23] de Juan F, Sturla M and Vozmediano M A H 2012 Space dependent Fermi velocity in strained graphene *Phys. Rev. Lett.* **108** 227205
[24] Yan H *et al* 2013 Superlattice Dirac points and space-dependent Fermi velocity in a corrugated graphene monolayer *Phys. Rev.* B **87** 075405
[25] Jang W-J, Kim H, Shin Y-R, Wang M, Jang S K, Kim M, Lee S, Kim S-W, Song Y J and Kahng S-J 2014 Observation of spatially-varying Fermi velocity in strained-graphene directly grown on hexagonal boron nitride *Carbon* **74** 139–45

[26] de Juan F, Cortijo A and Vozmediano M A H 2007 Charge inhomogeneities due to smooth ripples in graphene sheets *Phys. Rev.* B **76** 165409
[27] de Juan F, Mañes J L and Vozmediano M A H 2013 Gauge fields from strain in graphene *Phys. Rev.* B **87** 165131
[28] Volovik G E and Zubkov M A 2014 Emergent Horava gravity in graphene *Ann. Phys.* **340** 352–68
[29] Oliva-Leyva M and Naumis G G 2015 Generalizing the Fermi velocity of strained graphene from uniform to nonuniform strain *Phys. Lett.* A **379** 2645–51
[30] Luican A, Li G and Andrei E Y 2011 Quantized Landau level spectrum and its density dependence in graphene *Phys. Rev.* B **83** 041405
[31] Storz O *et al* 2016 Mapping the effect of defect-induced strain disorder on the Dirac states of topological insulators *Phys. Rev.* B **94** 121301
[32] Pereira V M, Neto A H C and Peres N M R 2009 Tight-binding approach to uniaxial strain in graphene *Phys. Rev.* B **80** 045401
[33] Luttinger J M 1951 The effect of a magnetic field on electrons in a periodic potential *Phys. Rev.* **84** 814–7
[34] Torres L F, Roche S and Charlier J-C 2014 *Introduction to Graphene-Based Nanomaterials* (New York: Cambridge University Press)
[35] Andrei E Y, Li G and Du X 2012 Electronic properties of graphene: a perspective from scanning tunneling microscopy and magnetotransport *Rep. Prog. Phys.* **75** 056501